Phase-excitation spectrum of ferroelectric liquid crystals in an external static electric field

B. Kutnjak-Urbanc[1] and B. Žekš[2]
[1]*Jožef Stefan Institute, University of Ljubljana, 61111 Ljubljana, Slovenia*
[2]*Institute of Biophysics, Medical Faculty, Lipičeva 2, 61105 Ljubljana, Slovenia*
(Received 10 May 1994; revised manuscript received 8 June 1995)

The dynamics of the phase of the molecular tilt in the helical ferroelectric liquid crystalline Sm-C^* phase is studied within the Landau model. We show that a static electric field applied parallel to smectic layers induces a gap in the excitation spectrum of the phase of the tilt at the edge of the Brillouin zone. The gap is shown to grow linearly with the strength of the field up to a critical field beyond which the helical structure finally unwinds. The influence of the phase-excitation dynamics on the dielectric response is investigated in order to resolve the contradiction between experimental findings and previous theoretical results. We find the dielectric strength of an infinitely large system to decrease with the bias field and go to zero at the critical field in accordance with measurements. In order to aquire a better understanding, the properties of a system of a finite length along the helical axis are investigated. It is shown that the dielectric strength consists of two parts: one related to the local variations of the phase of the tilt and the other related to the unwinding of the whole helical structure. The former part of the dielectric strength vanishes at the critical field, whereas the latter part diverges. In addition, the relaxation time for the unwinding of the helical structure is found to increase with the length of the system and has a range in real planar samples from minutes to hours. In conclusion, the dynamics of the tilt in a finite-size system is found to be crucial in interpreting experimental as well as theoretical results.

PACS number(s): 61.30.Gd, 64.70.Md, 64.70.Rh

I. INTRODUCTION

Ferroelectricity in liquid crystals was predicted in 1975 by Meyer *et al.* [1] for compounds with chiral molecules carrying transverse electric dipole moments, which order in a certain temperature regime into a tilted smectic phase. In the smectic liquid-crystalline phases, molecules are arranged into layers. In the smectic-C (Sm-C) phase the molecular director is tilted with respect to the normal to the smectic layers. If constituent molecules are chiral, the corresponding tilted smectic phase is called a smectic-C^* (Sm-C^*) phase.

In the chiral ferroelectric Sm-C^* phase the molecular tilt rotates around the normal to smectic layers as we proceed from one layer to another. As a consequence of this rotation, a helical structure is formed with a period, i.e., the helical pitch, on the order of thousands of smectic layers [2]. An external magnetic or electric field applied parallel to the smectic layers couples to the local molecular director [3] and deforms the helical structure. Such a field breaks the continuous helical symmetry and induces a discrete periodic lattice along the helical axis, usually referred to as the soliton lattice [4]. The lattice constant of the soliton lattice increases with the field and diverges at the critical field. At the critical field the helical structure unwinds and the phase transition to the homogeneously tilted Sm-C phase occurs. Rigorous theoretical studies [5] of the static properties of this soliton lattice show that the structure can be described well using the constant amplitude approximation (CAA), i.e., by the phase of the two-component order parameter tilt $\vec{\xi}$, neglecting the variations of the amplitude of the tilt. However, the CAA is not valid close to T_c ($T_c - T < 0.1$ K). By T_c we denote the transition temperature from the high-temperature smectic-A (Sm-A) phase to the Sm-C^* phase.

In the Sm-A phase, where the molecular director is perpendicular to smectic layers, only fluctuations of the amplitude of the tilt contribute to the low-frequency excitation spectrum. At the Sm-A↔Sm-C^* phase transition, the spectrum splits into two branches [6]: one corresponding to excitations of the tilt amplitude and the other to fluctuations of the phase of the tilt. Experiments show that by excluding a narrow temperature region below T_c, amplitude excitations can be neglected in comparison to phase excitations [7].

In this paper we investigate excitations of the phase of the tilt in an external static electric field. In Sec. II we show that the field induces a gap in the spectrum of excitations of the phase of the tilt at the edge of the Brillouin zone. The gap is shown to grow linearly with the field. The eigenmodes of these excitations are studied for wave vectors at the center and at the edge of the Brillouin zone. Preliminary experimental results, obtained by using light scattering methods, show the possibility of the existence of the gap in the phase-excitation spectrum at the edge of the Brillouin zone [8].

Phase excitations influence the dielectric response especially away from T_c, where the amplitude excitations can be neglected. The measured dielectric strength decreases with the bias field and vanishes at the critical field [9]. According to early theoretical predictions by

1063-651X/95/52(4)/3892(12)/$06.00

Hudák [10], the static susceptibility diverges at the critical field, which is in discrepancy with the experimental results. Motivated by this lack of agreement, we present in Sec. II our numerical results for the dielectric susceptibility, which qualitatively agree with the experimental findings.

To understand the difference between the predictions given by Hudák and our present results described in Sec. II, we study in Sec. III the influence of a finite system length on the phase-excitation spectrum and the contribution of the phase fluctuations to the dielectric response [11]. We find that the susceptibility consists of two contributions: one associated with the local reorientation of the tilt and the other related to the unwinding of the helical structure that affects the whole system [12]. The unwinding of the helical structure is argued to be crucial in understanding the results of dielectric measurements as well as in interpreting theoretical calculations. We then conclude that the slow dynamics of the unwinding of the helical structure is the reason for the discrepancy between the theory and measurements regarding the order of the Sm-$C^*\leftrightarrow$ Sm-C phase transition induced by the external field [4].

II. PHASE-EXCITATION SPECTRUM OF AN INFINITELY LARGE SYSTEM IN A STATIC ELECTRIC FIELD

In a system that is not in equilibrium a thermodynamic force appears, which drives the system back to the equilibrium. In this section we derive the equation that governs the dynamics of the phase of the tilt $\vec{\xi}$ around its equilibrium in a static electric field. The excitations are studied as well as the influence of the field on the static dielectric response.

The tilt $\vec{\xi}$ and the polarization $\vec{P}$ are expressed in terms of magnitudes Θ, P and the phase Φ: $\vec{\xi}=\Theta(\cos\Phi,\sin\Phi)$ and $\vec{P}=P(-\sin\Phi,\cos\Phi)$. Within the CAA only the phase Φ is allowed to vary, whereas the magnitudes Θ and P are kept constant. The relevant part of the Landau free energy per unit area is

$$\mathcal{F}=\int_{-\infty}^{+\infty}\left[\frac{1}{2}K_3\Theta^2\Phi'^2-K_3\Theta^2q_0\Phi'-EP\cos\Phi\right]dz. \tag{1}$$

By K_3 we denote an elastic constant and by $q_0=2\pi/p_0$ the wave vector of the helical pitch p_0 in a zero field. We choose the z axis to be parallel to the helical axis. Only the linear ferroelectric coupling between the polarization $\vec{P}$ and the field $\vec{E}=(0,E)$ is taken into account, whereas the quadratic coupling due to a dielectric anisotropy is neglected.

The dynamics of small fluctuations of the order parameter around the equilibrium is governed by Landau-Khalatnikov equations [13]. Within the CAA the Landau-Khalatnikov equations reduce to one equation for the phase $\Phi(z,t)$

$$K_3\Theta^2\frac{\partial^2\Phi}{\partial z^2}-EP\sin\Phi=\gamma\Theta^2\frac{\partial\Phi}{\partial t}, \tag{2}$$

where γ is a rotational viscosity. After introducing dimensionless variables for the coordinate $\tilde{z}=\pi q_0 z/4$, the time $\tilde{t}=(\pi/4)^2\gamma^{-1}K_3q_0^2t$, and the field $\sigma=E/E_c$, where $E_c=(\pi/4)^2K_3\Theta^2q_0^2/P$ is the critical field at which the Sm-$C^*\leftrightarrow$ Sm-C phase transition takes place, Eq. (2) is expressed in a dimensionless form

$$\Phi_{\tilde{z}\tilde{z}}-\sigma\sin\Phi=\Phi_{\tilde{t}}. \tag{3}$$

As we are interested in small fluctuations of the phase $\Phi(\tilde{z},\tilde{t})$ around the equilibrium, we write the solution $\Phi(\tilde{z},\tilde{t})$ of the nonlinear partial differential Eq. (3) as a sum of a static solution $\Phi_0(\tilde{z})$ and a small fluctuating part $\varphi(\tilde{z},\tilde{t})$, $\Phi(\tilde{z},\tilde{t})=\Phi_0(\tilde{z})+\varphi(\tilde{z},\tilde{t})$. The static equilibrium solution $\Phi_0(\tilde{z})$ for a given field E is a periodic solution of the sine-Gordon equation [14], which is expressed in terms of the Jacobi elliptic sine function

$$\Phi_0(\tilde{z})=\arccos\{2\mathrm{sn}^2[\sqrt{\sigma}\tilde{z}/k-K(k);k]-1\}. \tag{4}$$

The modulus $k\in[0,1]$ is related to the field σ through the equation $k=\sqrt{\sigma}E(k)$ and $K(k),E(k)$ are complete elliptic integrals of the first and the second kind, respectively. The modulated equilibrium state determined by Eq. (4) is periodic with a dimensionless period $\tilde{p}$, which depends on the reduced bias field σ, $\tilde{p}=2kK(k)/\sqrt{\sigma}$.

After linearizing Eq. (3) around the equilibrium solution $\Phi_0(\tilde{z})$, the equation for $\varphi(\tilde{z},\tilde{t})$ is obtained

$$\varphi_{\tilde{z}\tilde{z}}-\sigma\cos(\Phi)\varphi=\varphi_{\tilde{t}}. \tag{5}$$

According to Eq. (5) the system approaches on equilibrium exponentially and thus $\varphi(\tilde{z},\tilde{t})$ can be written as a product $\varphi(\tilde{z},\tilde{t})=\varphi_0(\tilde{z})\exp(-\tilde{t}/\tilde{\tau})$, where $\tilde{\tau}$ is a dimensionless characteristic time associated with the excitation. The problem of solving Eq. (5) is an eigenvalue one. Different eigenfunctions φ_0 correspond to different eigenvalues $k^2(1+\sigma^{-1}\tilde{\tau}^{-1})$ through the equation

$$\frac{d^2\varphi_0(\alpha)}{d\alpha^2}=[2k^2\mathrm{sn}^2(\alpha;k)-k^2(1+\sigma^{-1}\tilde{\tau}^{-1})]\varphi_0(\alpha). \tag{6}$$

We introduced a new independent variable $\alpha=\sqrt{\sigma}\tilde{z}/k-K(k)$. The relaxation frequencies $\tilde{\tau}^{-1}$, which determine the phase-excitation spectrum, are directly related to the eigenvalues $k^2(1+\sigma^{-1}\tilde{\tau}^{-1})$.

A. Field-induced gap

Equation (6) is the Lamé equation of first order [15]. It is of the same form as a stationary Schrödinger equation in one dimension for a particle in a periodic elliptic potential. This equation is not rare in condensed matter physics: it describes small fluctuations of a flux-line lattice in superconductors of type II [16], phase-excitations in cholesterics [17], and also excitations of ferroelectric liquid crystals in an external magnetic field [18]. The solutions of this equation are expressed in terms of the

Jacobi eta $H(\alpha;k)$, theta $\Theta(\alpha;k)$, and zeta $Z(\alpha;k)$ functions

$$\varphi_0(\alpha;\alpha_0;k) = \frac{H(\alpha+\alpha_0;k)}{\Theta(\alpha;k)} \exp[-\alpha Z(\alpha_0;k)], \quad (7)$$

whereas the eigenvalues determine the eigenfrequencies $\tilde{\tau}^{-1}$ through the relation

$$\tilde{\tau}^{-1} = \frac{\sigma}{k^2} dn^2(\alpha_0;k). \quad (8)$$

By $\mathrm{dn}(\alpha;k)$ we denote the Jacobi elliptic delta function. The parameter α_0 is an index that plays the role of a wave vector, i.e., it determines the wavelength of the excitation. Equation (8) is a dispersion relation that determines the phase-excitation spectrum at a given field σ.

As the potential in the Schrödinger-like equation (6) is periodic, the solution $\varphi_0(\alpha;\alpha_0;k)$ that describes the phase excitation must have Bloch form. The argument of the exponent in Eq. (7) thus has to be imaginary, i.e., $iq_\alpha\alpha$, where q_α is a wave vector, inversely proportional to the wavelength of the excitation λ, $q_\alpha = 2\pi/\lambda$. Each phase excitation is characterized by the wave vector q_α, so that the corresponding Bloch function can be denoted by $\Psi_{q_\alpha}(\alpha)$ instead of $\varphi_0(\alpha;\alpha_0;k)$. In the following the Bloch form $\Psi_{q_\alpha}(\alpha)$ will be used. By taking into account the properties of Bloch functions under the translation for a lattice constant $\alpha_T = 2K(k)$ on one side and the translational properties of the Jacobi functions [19] $H(\alpha;k)$, $\Theta(\alpha;k)$, and $Z(\alpha;k)$ on the other, we find the relationship between the complex parameter α_0 and the wave vector q_α

$$q_\alpha = \pm\frac{1}{2}q_{\alpha,c} - iZ(\alpha_0). \quad (9)$$

Here $q_{\alpha,c} = 2\pi/\alpha_T = \pi/K(k)$ is the dimensionless critical wave vector associated with the lattice constant α_T in a real space. The double sign in Eq. (9) reflects the translational invariance in the reciprocal space for the critical wave vector $q_{\alpha,c}$. In the following we choose the Brillouin zone corresponding to $q_\alpha \in [q_{\alpha,c} - q_{\alpha,c}/2, q_{\alpha,c} + q_{\alpha,c}/2]$. In order to obtain real values of q_α the parameter α_0 should be chosen in such a way as to yield an imaginary value for $Z(\alpha_0)$. The zeta function $Z(\alpha;k)$ is quasiperiodic, i.e., it is periodic in a real argument with the period $2K(k)$ and it is a monotonic function of an imaginary argument. The values of $Z(\alpha_0)$ are imaginary in two cases: (a) when $\alpha_0 = iy$ or (b) when $\alpha_0 = K(k) + iy$. Here y is a real parameter. These two cases determine two relaxation frequency bands and the gap in between. The gap splits the phase-excitation spectrum into two branches: (a) the upper opticlike branch and (b) the lower acousticlike branch. The gap appears at the edge of the Brillouin zone at the wave vectors $q_\alpha = q_{\alpha,c} \pm q_{\alpha,c}/2$. The phase-excitation spectrum and its splitting in the external static electric field are shown schematically in Fig. 1.

Both branches are depicted in Fig. 2 for a few different values of the bias field $\sigma = E/E_c$. The gap at $q = q_c \pm q_c/2$ increases linearly with the field, as shown in Fig. 3, where in addition to the gap Δ the relaxation frequencies

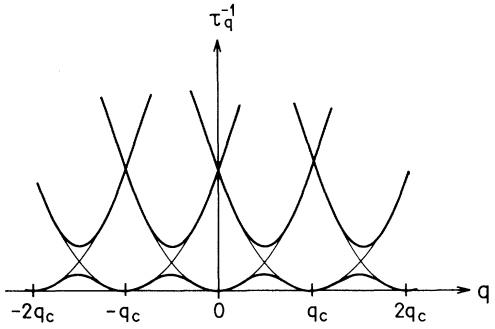

FIG. 1. The phase-excitation spectrum in an external electric field is shown schematically in an extended zone presentation. The two branches are separated by the gap at $q = \pm q_c/2, \pm 3q_c/2, \ldots$.

of the acousticlike and opticlike excitation with $q = q_c \pm q_c/2$ are depicted.

In a zero field the phase-excitation spectrum is parabolic with the center at $q = q_0$. The phase excitation in the center corresponds to the zero-frequency Goldstone mode: such an excitation describes a rigid rotation of the helix as a whole or a sliding of the helix along the z axis. The width of the Brillouin zone goes to zero continuously as the field approaches its critical value. Although the field breaks the continuous helical symmetry, there is still an excitation with a zero relaxation frequency in the center of the Brillouin zone, at $q = q_c$. This zero-frequency mode is a consequence of a continuous degeneracy of the modulated phase: the translation of domain walls along the helical axis does not change the free energy of the system. The existence of the zero-frequency excitation mode below the critical field can be predicted without calculations using merely symmetry arguments. The homogeneously tilted Sm-C phase above the critical field

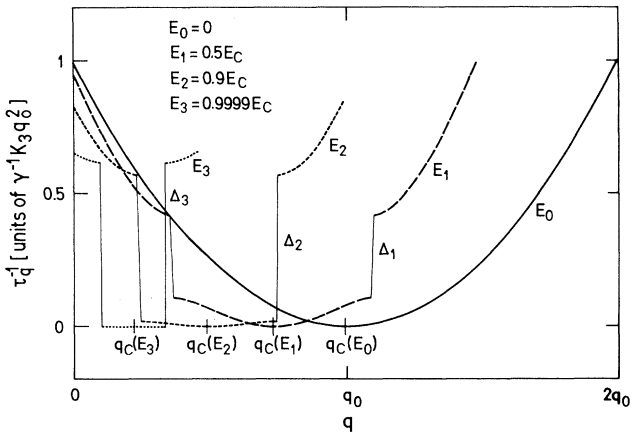

FIG. 2. Spectrum of phase excitations in an external static electric field that is perpendicular to the helical axis. Four different curves correspond to four different field strengths. The width of the zone goes to zero as the field approaches the critical field value. The gap at $q = q_c \pm q_c/2$ splits the phase-excitation spectrum into the lower acousticlike and the upper opticlike branch.

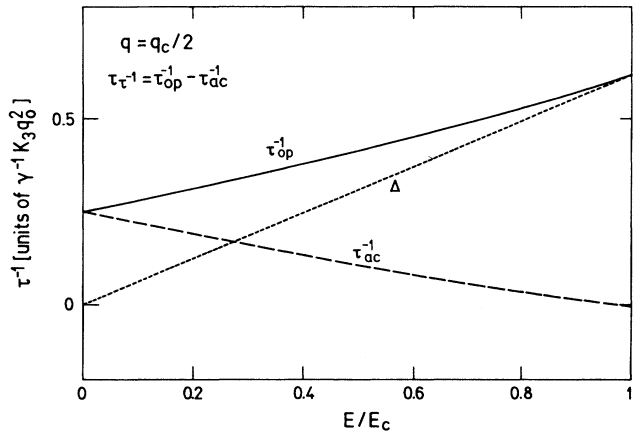

FIG. 3. Relaxation frequencies τ_{ac}^{-1} and τ_{op}^{-1} of the phase excitations with the wave vector $q = q_c \pm q_c/2$. Their difference $\Delta = \tau_{op}^{-1} - \tau_{ac}^{-1}$ represents the gap in relaxation frequencies, which is proportional to the field and assumes its maximal value $(\pi/4)^2\gamma^{-1}K_3q_0^2$ at the critical field.

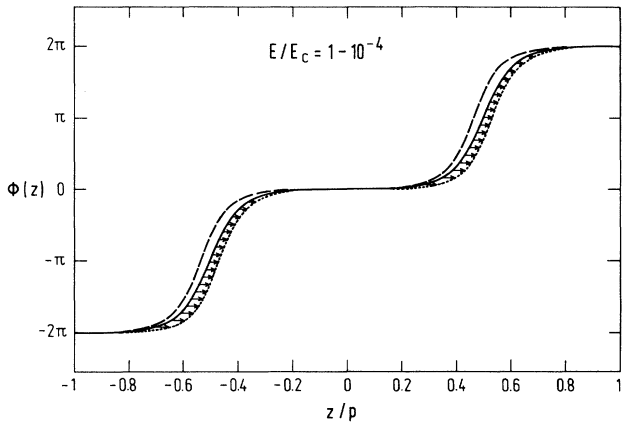

FIG. 4. Excitation on the acousticlike branch with the wave vector $q = q_c$ corresponds to a homogeneous translation of domain walls along the helical axis. The associated relaxation frequency is equal to zero at all field strengths below the critical one.

has a continuous translational symmetry apart from the discrete structure due to smectic ordering. On lowering the field from above to below the critical field the continuous translational symmetry is spontaneously broken and only a discrete translational invariance due to the soliton lattice remains. Therefore, in the Sm-C^* phase below the critical field a Goldstone-like [20], zero-frequency mode should exist, whereas in the Sm-C phase there can be only opticlike phase excitations with nonzero relaxation frequencies. The branch of phase excitations is in this sense analogous to spin density waves in an isotropic Heisenberg ferromagnet where the continuous rotational symmetry is broken in the low-temperature phase.

B. Eigenmodes of phase-excitations

What kind of an excitation corresponds to the complex Bloch function in a real space? The Bloch function $\Psi_{q_\alpha}(\alpha)$ and its complex conjugate $\Psi^*_{q_\alpha}(\alpha)$ are both solutions of the Lamé equation (6) with a real elliptic potential. Since the Lamé equation is linear, two linear combinations $\Psi^+_{q_\alpha} = (\Psi_{q_\alpha} + \Psi^*_{q_\alpha})/2$ and $\Psi^-_{q_\alpha} = (\Psi_{q_\alpha} - \Psi^*_{q_\alpha})/2i$ will also solve Eq. (6). These two real functions describe two phase excitations on a given branch with the wave vector q_α. The two phase excitations could hypothetically be induced by an electric field (the field could be oriented parallel or perpendicular to the bias field), which is modulated sinusoidally (with a period $2\pi/q_\alpha$) along the helical axis. The two excitations thus change the in-plane polarization parallel and perpendicular to the bias field, respectively.

There are three special points in the phase-excitation spectrum where the Bloch function is real: at the center of the Brillouin zone $q = q_c$ and at the edges of the Brillouin zone $q = q_c \pm q_c/2$. The acousticlike phase excitation with $q = q_c$ corresponds to a rigid translation of domain walls along the helical axis, as shown in Fig. 4. The corresponding Bloch function is proportional to the Jacobi elliptic delta function $\Psi^{ac}_{q_{\alpha,c}} \propto \mathrm{dn}(\alpha;k)$. The acousticlike phase excitation with $q = q_c \pm q_c/2$, which is presented in Fig. 5, corresponds to shifts of the two neighboring domain walls: as one wall moves to the left, the other one moves to the right. The domain between the two walls grows while the neighboring domain shrinks. It is not difficult to see that this excitation changes the local polarization along the bias field. The corresponding Bloch function is proportional to the Jacobi elliptic cosine function, $\Psi^{ac}_{q_{\alpha,c}\pm q_{\alpha,c}/2} \propto \mathrm{cn}(\alpha;k)$. The opticlike phase excitation with $q = q_c \pm q_c/2$ is depicted in Fig. 6. This excitation changes the width of domain walls: as one wall gets wider the neighboring one becomes narrower. The in-plane polarization perpendicular to the bias field is changed and the corresponding Bloch function is proportional to the Jacobi elliptic sine function, $\Psi^{op}_{q_{\alpha,c}\pm q_{\alpha,c}/2} \propto \mathrm{sn}(\alpha;k)$.

The eigenmodes in the three special points of the phase-excitation spectrum are analogous to the eigen-

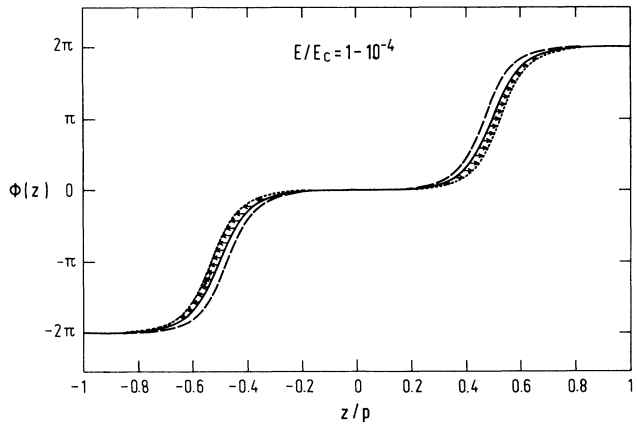

FIG. 5. Excitation on the acousticlike branch with the wave vector $q = q_c \pm q_c/2$: the positions of the two neighboring domain walls are shifted in opposite directions.

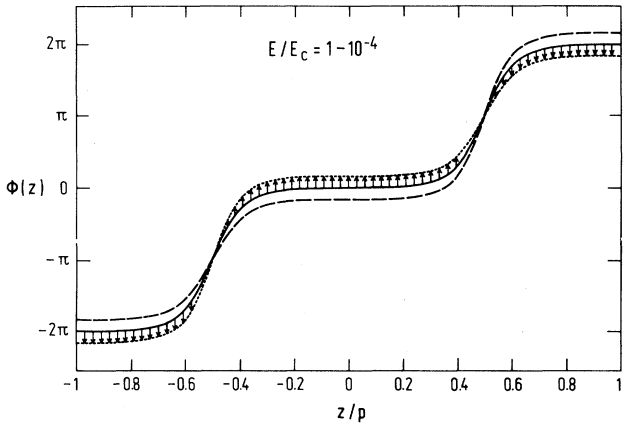

FIG. 6. Excitation on the opticlike branch with $q = q_c \pm q_c/2$. The widths of the domains are altered. As one domain gets wider, the neighboring one shrinks.

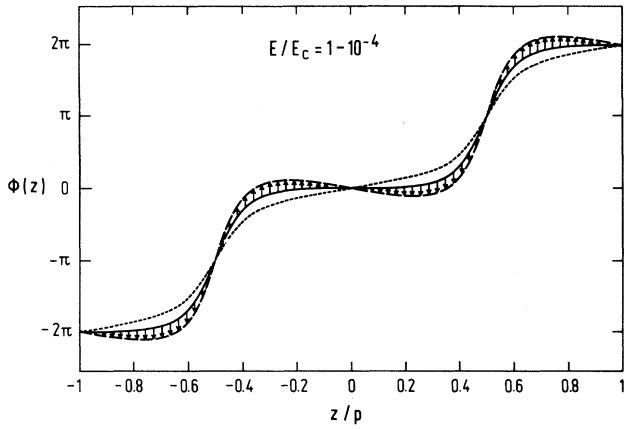

FIG. 7. Excitation on the opticlike branch with the wave vector $q = 0$. Such a phase-excitation mode can be excited by applying an electric field parallel to the static bias field.

modes in the phonon spectrum of a diatomic linear chain of identical atoms connected by springs of alternating strengths: one soft and the other hard [21]. Stretching the soft springs corresponds to changing of the width of domains and stretching the hard springs is related to varying the domain walls' widths. The corresponding zero-frequency mode is associated in this case with a homogeneous translation of the whole chain of springs and atoms.

C. Dielectric response in a bias electric field

Here the dielectric response of an infinitely large system to a time-dependent field applied either parallel or perpendicularly to the static bias field is investigated. In an external static electric field only the phase excitations with wave vectors $q = 0, \pm q_c, \pm 2q_c, \ldots$ influence the dielectric response. The acousticlike phase excitation with $q = q_c$ does not affect the average polarization of the system because it represents the translation of the lattice as a whole and thus cannot contribute to the response. The main contribution is expected from an opticlike excitation with $q = 0$. The contributions from opticlike excitations with $q = 2q_c, 3q_c, \ldots$ can be neglected since their relaxation frequencies are higher and the contributions correspondingly smaller.

The two opticlike phase excitations with $q = 0$ are shown in Figs. 7 and 8: they can be excited by a small homogeneous field that is parallel and perpendicular to the bias field, respectively. The corresponding relaxation frequency, which is the same for both excitations, is depicted in Fig. 9 in dependence on the bias field. This frequency is almost unaltered at small bias fields and is slightly lowered as the field approaches its critical value, where it assumes $(\pi/4)^2 \approx 0.79$ of its zero field value. At fields higher than the critical one the relaxation frequency increases linearly with the field.

Knowing the Bloch functions of the opticlike phase excitation with $q = 0$, we can calculate the dielectric strength of the response in dependence on the bias field. The results are presented in Fig. 10. The static dielectric response to a small field that is applied parallel to the bias field decreases with the bias field. At the critical field where the polarization in each layer is parallel to the bias field, the additional field does not induce any polarization along the bias field and consequently the dielectric strength at the critical bias field is zero. The static dielectric response to a small field that is applied perpendicularly to the bias field increases with the field. In this case the response is proportional to an average polarization along the bias field that grows with the field up to the critical field. Above the critical field both responses are independent of the bias field.

According to the above results the static dielectric response to a small field that is parallel to the bias field decreases with the bias field, which is in agreement with measured data [9]. This, however, contradicts the static susceptibility, which has been shown by Hudák [10] to diverge logarithmically at the critical field. In his calculation the dynamic behavior of the system was not taken

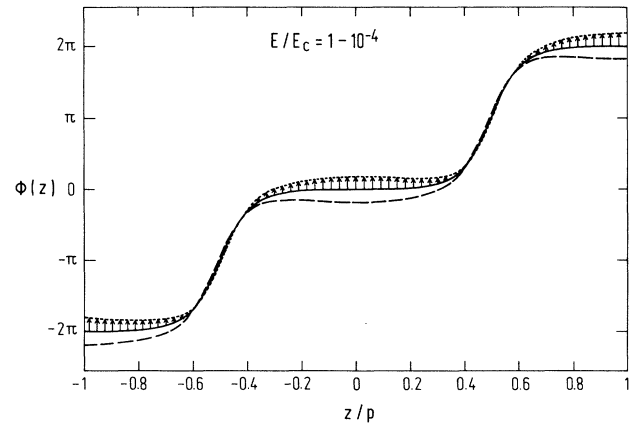

FIG. 8. Excitation on the opticlike branch with the wave vector $q = 0$. Such a phase-excitation mode can be excited by applying an electric field perpendicular to the static bias field.

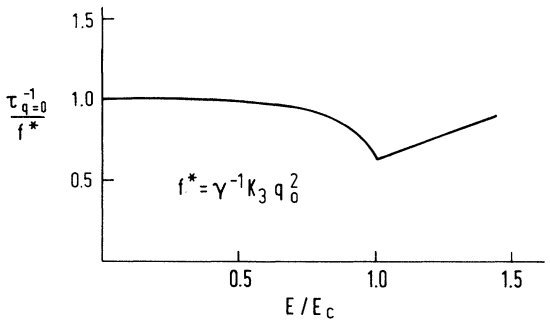

FIG. 9. The relaxation frequency, which is associated with the opticlike phase excitations with $q = 0$, is depicted as a function of the bias electric field.

into account and the strong increase of the static susceptibility below the critical field is a result of the variation of the helical pitch under the influence of the field change. On the other hand, it was noted by the author himself that in a macroscopically large system the change of the helical period requires large rotations of the director. In the following we will show that in an infinitely large system the phase excitation that corresponds to the unwinding of the helical structure should have an infinite relaxation time.

III. EFFECTS OF FINITE DIMENSIONS

Results of the preceding section are based on the investigation of phase excitations in an infinitely large system, whereas in experiments the sample is always finite along the helical axis. The helical period in such a finite system in dependence on the field has been shown recently to exhibit finite jumps [11] at some field values where the number of domain walls in the sample is changed by one. However, in a system that is large enough, a discontinuous field behavior of the period is less pronounced

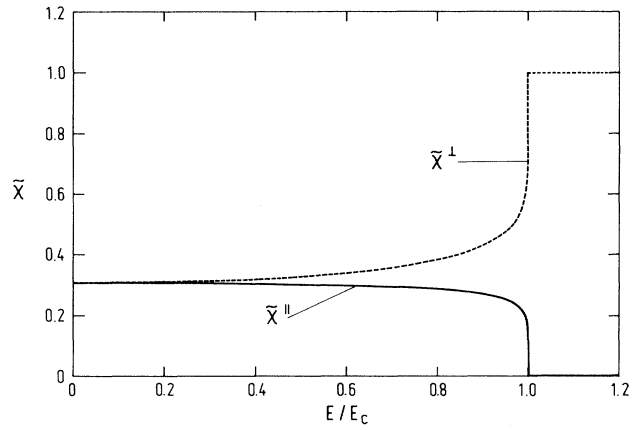

FIG. 10. A static dielectric response as calculated numerically in dependence on the strength of the bias electric field is presented in two cases: when an additional field is parallel to the bias field ($\tilde{\chi}^{\parallel}$) and when an additional field is perpendicular to the bias field ($\tilde{\chi}^{\perp}$).

and the curve practically agrees with the result for an infinitely large system. Although the static behavior of a thick sample is almost the same as in an infinite system, the dynamical behavior is expected [12] to be influenced essentially by finite dimensions.

A. Dielectric response of a finite system in a zero bias field

In order to understand the dynamical behavior of a finite sample, its dielectric response in a zero bias field is studied. A system of finite length along the helical axis is polarized unless there is exactly an integer number of helical periods in the system. In the absence of external fields we denote the dipole moment of the sample by $\vec{p}$. Here we investigate the dielectric response of a system to a time-dependent electric field $\delta\vec{E} = \delta\vec{E}_0 \cos\omega t$ applied perpendicularly to the helical axis. The derivation of the dielectric susceptibility in dependence on the field frequency is given in the Appendix. The dielectric susceptibility is a 2×2 tensor and the two eigenvalues are given by Eqs. (A11)–(A13). The eigenvalues $\chi^{\parallel}$ and $\chi^{\perp}$ correspond to the complex susceptibilities that measure the linear response to a time-dependent field applied parallel ($\delta\vec{E} \parallel \vec{p}$) and perpendicularly ($\delta\vec{E} \perp \vec{p}$) to the dipole moment $\vec{p}$, respectively. The last term in Eq. (A11), which gives $\chi^{\perp}_{\mathrm{Re}} \propto \delta(\Omega)$ and $\chi^{\perp}_{\mathrm{Im}} \propto 1/\Omega$ [a dimensionless frequency $\Omega = \gamma\omega/(K_3 q_0^2)$], corresponds to a rigid rotation of the helix as a whole. This contribution disappears only when $L = kp_0$, with k being an integer, i.e., when the total static dipole moment $\vec{p}$ vanishes. This part of the response of the system can be understood in the following way. The nonzero dipole moment $\vec{p}$ breaks the axial symmetry in the smectic plane in comparison to the case $\vec{p} = \vec{0}$. The presence of this additional zero-frequency relaxation mode can be predicted on the basis of the Goldstone theorem [20] as a consequence of the broken (continuous) axial symmetry.

As shown in the Appendix, the sums in Eqs. (A11) can be expressed explicitly by evaluating partial sums separately. In Figs. 11 and 12 the results for both responses, $\chi^{\parallel}_{\mathrm{Re}}, \chi^{\parallel}_{\mathrm{Im}}$ and $\chi^{\perp}_{\mathrm{Re}}, \chi^{\perp}_{\mathrm{Im}}$, are depicted for four different lengths L of the system in dependence on the field frequency. All the lengths L are chosen in such a way that the total dipole moment is fixed in order to study only the effect of the system length L along the helical axis. The peaks in $\chi^{\parallel}_{\mathrm{Im}}$ and $\chi^{\perp}_{\mathrm{Im}}$ appear at two different characteristic frequencies: (a) at $\omega_0 = \gamma^{-1} K_3 q_0^2$, which is associated with a relaxation at a constant pitch, and (b) at $\omega_1 = \gamma^{-1} K_3 q_{\mathrm{min}}^2$, which is associated with the unwinding of the helical structure. The wavelength λ that corresponds to $q_{\mathrm{min}} = 2\pi/\lambda$ is the largest wavelength allowed in a system of the length L. For the field $\delta\vec{E} \parallel \vec{p}$ the smallest allowed wave vector is $q^{\parallel}_{\mathrm{min}} = \pi/L$, while in the case $\delta\vec{E} \perp \vec{p}$ the smallest wave vector is $q^{\perp}_{\mathrm{min}} = 2\pi/L$. This can be noticed by analyzing the expressions (A11) and it can be observed on comparing Figs. 11 and 12 ($\omega^{\parallel}_1 = \omega^{\perp}_1/4$). In both cases the relaxation frequency ω_1 depends on the length L of the system: as the length

L of the system increases, the relaxation frequency ω_1 decreases as $\omega_1 \propto L^{-2}$.

An interesting question is what happens to the complex susceptibility $\chi_{\rm Re} + i\,\chi_{\rm Im}$ as the length L gets larger and larger. In the following only the response to the field that is parallel to $\vec{p}$ is studied. The results obtained by taking the limit $L \to \infty$ at $\Omega > 0$ of the expression for $\chi^{\parallel}$ in Eq. (A12) yield

$$\chi_{\rm Re} = \frac{\pi^2}{32}\frac{P}{E_c}\frac{1}{1+\Omega^2}, \qquad \chi_{\rm Im} = \frac{\pi^2}{32}\frac{P}{E_c}\frac{\Omega}{1+\Omega^2}, \tag{10}$$

where the superscripts are omitted. This is exactly the result of an infinite system at fixed helical period, so that only the contribution at $\Omega = 1$ (at $\omega = \omega_0$) is present. In the case $\Omega = 0$, which has to be treated separately, there are additional contributions to $\chi_{\rm Re}$ and $\chi_{\rm im}$ that depend on the dimensionless length $l = 2L/p_0$. By assuming that the dimensionless length l is very large but still finite, we find

$$\chi_{\rm Re}(\Omega \to 0) \approx \frac{P}{E_c}\frac{\pi^2}{32}[1 + 2\cos^2(\pi l/2)],$$

$$\frac{\chi_{\rm Im}}{\Omega}(\Omega \to 0) \approx \frac{P}{E_c}\left\{\frac{\pi^2}{32}[1 + 4\cos^2(\pi l/2)] + \frac{\pi^4 l^2}{192}\cos^2(\pi l/2)\right\}. \tag{11}$$

In the limit $l \to \infty$ the last term in $\chi_{\rm Re}$ remains finite while the last term in $\chi_{\rm Im}/\Omega$ diverges. From Eqs. (A11)–(A13) we derive the rigorous expression for the real part of the susceptibility of an infinite system

$$\chi_{\rm Re}(\Omega) = \frac{P}{E_c}\frac{\pi^2}{32}\left[\frac{1}{1+\Omega^2} + \tilde{\chi}_0\right], \tag{12}$$

where the last contribution $\tilde{\chi}_0 = 2\lim_{l\to\infty}\cos^2(\pi l/2)$ is nonzero only at the zero frequency $\Omega = 0$. Using the Kramers-Krönig relation [13] between the real and the imaginary part of the susceptibility we find

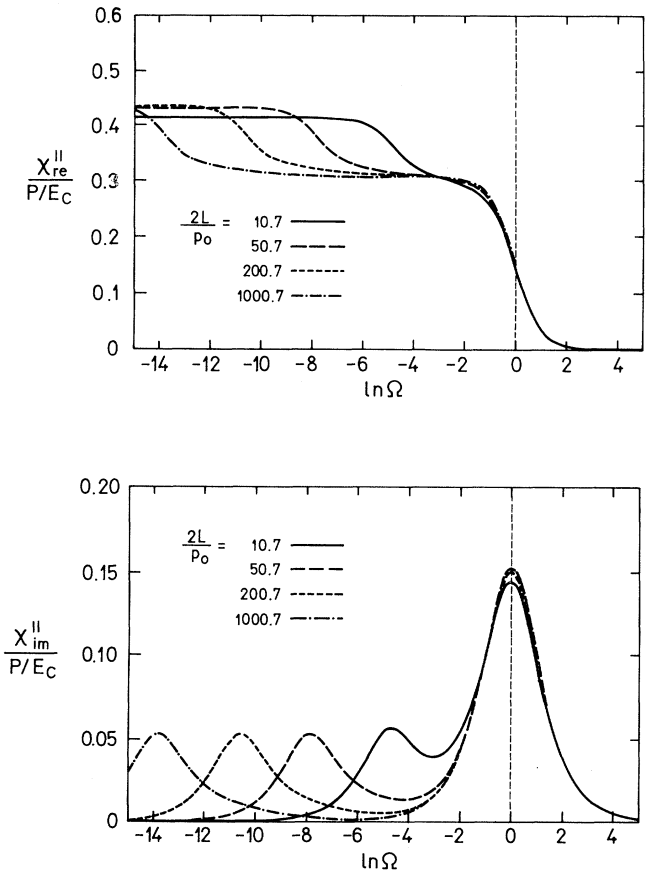

FIG. 11. The real and the imaginary part of the complex susceptibility, which measures the response to the time-dependent field applied parallel to the dipole moment $\vec{p}$, are shown in dependence on the frequency of the field. Different curves correspond to different lengths L of the system: $2L/p_0 = 10.7, 50.7, 200.7$, and 1000.7.

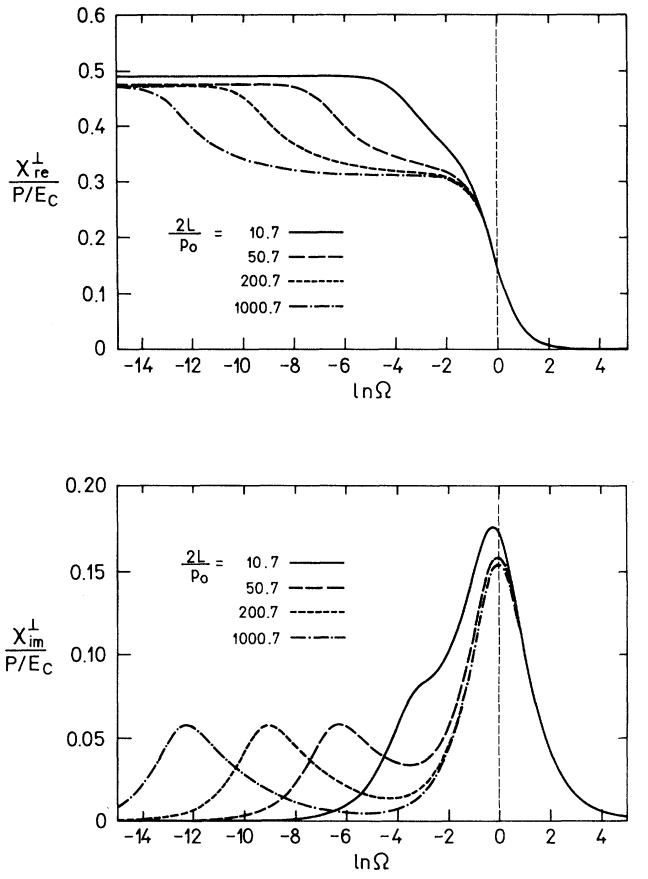

FIG. 12. The real and the imaginary part of the complex susceptibility, which measures the response to the time-dependent field applied perpendicularly to the dipole moment $\vec{p}$, are shown in dependence on the frequency of the field. Different curves correspond to different lengths L of the system: $2L/p_0 = 10.7, 50.7, 200.7$, and 1000.7.

$$\chi_{\mathrm{Im}}(\Omega) = \frac{P}{E_c}\frac{\pi^2}{32}\left[\frac{\Omega}{1+\Omega^2} + \frac{\pi}{2}\tilde{\chi}_0\,\Omega\delta(\Omega)\right]. \quad (13)$$

The limit $l \to \infty$ should be taken at a fixed value of the total dipole moment $\vec{p}$ of the system: the number of periods in the system is increased in such a way that the value of $\cos^2(\pi l/2)$ is unaltered.

In a system of infinite length along the helical axis the phase-excitation mode that unwinds the helical structure cannot be excited in a finite time. The zero relaxation frequency mode derived above is not a consequence of a vanishingly small thermodynamic force as it is in the case of soft and Goldstone modes, but it is a result of infinitely large rotations of the director needed to unwind the helical structure.

B. Phase-excitation spectrum of a finite system

The problem of the phase-excitation spectrum of a finite system is analogous to the problem of the phonon spectrum of a finite crystal. In an infinitely large crystal the phonon excitations with all wavelengths contribute to the spectrum: the spectrum is continuous. In a finite crystal one usually applies periodic boundary conditions for Bloch functions that describe phonon excitations. Since not all phonon excitations satisfy the boundary conditions, only discrete values of phonon wavelengths are allowed: the spectrum is discrete. The phonon-excitation profiles with the allowed wave vectors are, however, the same as in an infinite crystal.

Our investigation of the dynamics of phase excitations in a system of finite length L along the helical axis is based on the Landau-Khalatnikov equation (2). We write the solution $\Phi(\tilde{z},\tilde{t})$ of the dimensionless equation (3) as a sum of the static solution [11] $\Phi_0(\tilde{z})$ at a given reduced field σ and the fluctuating part, which can be expressed as $\varphi_0(\tilde{z})\exp(-\tilde{t}/\tilde{\tau})$, so that we obtain the following equation for the amplitude $\varphi_0(\tilde{z})$:

$$\varphi_0''(\tilde{z}) = [\sigma\cos\Phi_0 - \tilde{\tau}^{-1}]\,\varphi_0(\tilde{z}). \quad (14)$$

The potential in the Schrödinger-like equation (14) is defined for $\tilde{z} \in [-\tilde{L}/2, +\tilde{L}/2]$ where $\tilde{L}$ is a dimensionless length of the system $\tilde{L} = \pi q_0 L/4$. The equilibrium phase profile $\Phi_0(\tilde{z})$ that determines the form of the potential describes a periodic structure with a dimensionless period $\tilde{p}_L = 2\kappa K(\kappa)/\sqrt{\sigma}$ and can be expressed as

$$\cos(\Phi_0/2) = \mathrm{sn}[\sqrt{\sigma}(\tilde{z}+\tilde{z}_0)/\kappa;\kappa],$$

$$\tilde{z}_0 = \frac{\tilde{L}}{2} + \frac{\kappa}{\sqrt{\sigma}}F\left(\frac{\Phi_- + \pi}{2};\kappa\right), \quad (15)$$

where $\kappa = 2\sqrt{E}/[(4/\pi)^2 E_c + 4E\cos^2(\Phi_-/2)]$, Φ_- is the value of the phase at the lower free boundary, $\Phi_- = \Phi_0(\tilde{z} = -\tilde{L}/2)$, and E_c is the critical field of an infinitely large system. By introducing a new variable $\alpha = \sqrt{\sigma}(\tilde{z}+\tilde{z}_0)/\kappa$, Eq. (14) transforms to an equation that has the form of the Lamé equation except that the potential is defined on a finite interval only

$$\frac{d^2\varphi_0(\alpha)}{d\alpha^2} = [2\kappa^2\mathrm{sn}^2(\alpha;\kappa) - \kappa^2(1+\sigma^{-1}\tilde{\tau}^{-1})]\,\varphi_0(\alpha), \quad (16)$$

i.e., for $\alpha \in [\alpha_-, \alpha_+]$, where

$$\alpha_- = F\left(\frac{\Phi_- + \pi}{2};\kappa\right), \qquad \alpha_+ = \alpha_- + \frac{\sqrt{\sigma}}{\kappa}\tilde{L}. \quad (17)$$

The excitation with a given wave vector q_α on each of the two branches can be expressed as a linear combination of the two real solutions $\Psi^+_{q_\alpha}$ and $\Psi^-_{q_\alpha}$ of the Lamé equation, respectively,

$$\Phi_{q_\alpha}(\alpha) = A\Psi^-_{q_\alpha}(\alpha) + B\Psi^+_{q_\alpha}(\alpha). \quad (18)$$

The allowed wave vectors q_α are determined by the boundary conditions at α_- and α_+: the derivatives $d\Phi_{q_\alpha}(\alpha)/d\alpha$ are zero at both boundaries α_- and α_+. These two conditions, applied to the ansatz (18), lead to a system of two homogeneous linear equations for the coefficients A and B that can be solved if and only if the determinant of the system is zero

$$\left.\frac{d\Psi^+_{q_\alpha}}{d\alpha}\right|_{\alpha_-}\left.\frac{d\Psi^-_{q_\alpha}}{d\alpha}\right|_{\alpha_+} - \left.\frac{d\Psi^-_{q_\alpha}}{d\alpha}\right|_{\alpha_-}\left.\frac{d\Psi^+_{q_\alpha}}{d\alpha}\right|_{\alpha_+} = 0. \quad (19)$$

The above equation determines the discrete values of wave vectors that are allowed in the phase-excitation spectrum. This spectrum is presented in Fig. 13. The critical wave vector $q_c = 2\pi/p_L$ determines the width of the Brillouin zone. Its value depends on the bias field. Since the period p_L of the helix changes discontinuously, the critical wave vector also exhibits jumps at the same values of the field. Unless there is exactly an integer number of helical periods in the system, the excitations with $q = 0$ and $q = q_c \pm q_c/2$ (i.e., special points of the spectrum where the associated Bloch function is real) are not allowed in the phase-excitation spectrum of a finite system. The number of allowed wave vectors within the Brillouin zone of the width q_c is given approximately by $q_c/q_m = 2L/p_L$, where $q_m = \pi/L$ is the wave vector

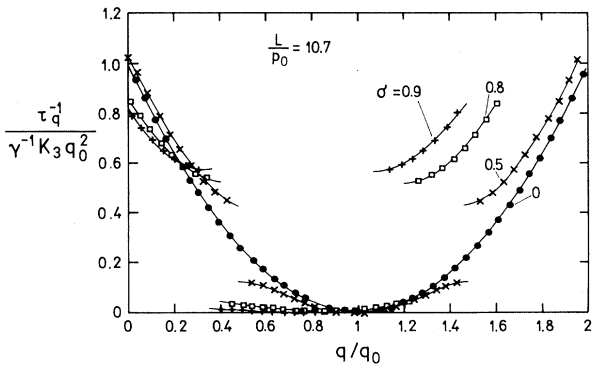

FIG. 13. The dispersion relation of phase excitations of a finite system with the length $L = 10.7p_0$ along the helical axis is discrete. The solid lines belong to an infinitely large system. Different curves correspond to different field strengths.

associated with the phase excitation of the largest wavelength.

C. Influence of finite dimensions on the dielectric response in a bias field

The contribution to the dielectric response from the phase excitation with the wave vector q_α is proportional to $(\int_0^{+L} \Psi_{q_\alpha} \cos\Phi_0 dz)^2$, where Ψ_{q_α} is the corresponding Bloch function. For a very large length L this integral is zero unless q_α matches the wave vector associated with the modulation of the equilibrium state. Thus, in the limit $L \to \infty$ only phase excitations with $q = 0, \pm q_c, \pm 2q_c, \ldots$ contribute to the response. On the other hand, the dielectric response of a finite system is influenced by all the allowed phase excitations. The major part of the contribution to the dielectric response, however, originates in the allowed phase-excitation modes with wave vectors closest to $q = 0, \pm q_c, \pm 2q_c, \ldots$. In a system with a length of many helical pitches, the main part of the dielectric response is determined by the lowest-frequency phase excitations: the opticlike excitation with the wave vector q from the interval $q \in [-\pi/L, +\pi/L]$ and the acousticlike excitation with the wave vector q from the interval $q \in [q_c - \pi/L, q_c + \pi/L]$. The phase excitation with $q \approx 0$ is associated with the local reorientation of the tilt and the in-plane polarization at a constant helical period. The phase excitation with $q \approx q_c$ changes the helical period, except in the special case when there is exactly an integer number of helical periods in the system. In this special case the excitation with $q = q_c$ is allowed, but since it only shifts the domain walls along the helical axis and does not affect the polarization of the system, it does not contribute to the response.

In an external bias field just below the critical field all the allowed phase excitations contribute to the dielectric response, since the system below the critical field consists of small number of helical periods. However, a characteristic time that the system needs to reach an equilibrium is determined by the phase excitation with the longest possible relaxation time. Such an acousticlike excitation is associated with the wave vector $q \approx q_c$ and changes the helical period. The corresponding relaxation frequency is depicted in Fig. 14(a) in dependence on the bias field at a few different lengths L of the system. The jumps that occur at some special field values are due to the jumps in the critical wave vector q_c. The relaxation frequency is lowered under the influence of the bias field and goes almost to zero at the critical field.

The phase-excitation frequency at $q \approx 0$ on the optic branch is presented in Fig. 14(b) as a function of the bias field. The observed jumps are due to the discontinuous behavior of the critical wave vector q_c. In contrast to the relaxation frequency in Fig. 14(a), the relaxation frequency in Fig. 14(b) does not depend much on the length L of the system apart from the discontinuous behavior which is more pronounced at smaller lengths L.

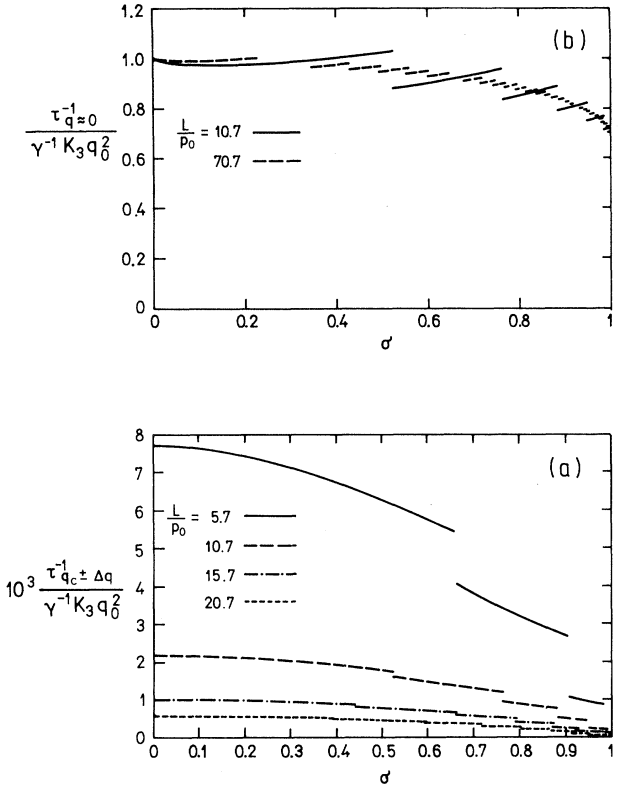

FIG. 14. (a) Relaxation frequency $\tau^{-1}_{q_c \pm \Delta q}$ of the excitation with the largest wavelength allowed in a system of a finite length L along the helical axis. Different curves correspond to different lengths L of the system. (b) Relaxation frequency $\tau^{-1}_{q \approx 0}$ of an opticlike excitation with the wavelength $q \approx 0$. Two different curves are presented, which correspond to two different lengths L.

IV. CONCLUSIONS

An external electric field applied parallel to the smectic layers in the liquid-crystalline Sm-C^* phase induces a one-dimensional lattice along the helical axis. In this paper we study excitations of the phase of the tilt of this soliton lattice to the lowest order. The phase-excitation spectrum is found to be equivalent to the energy spectrum of a particle moving in a one-dimensional periodic elliptic potential. It is shown that the field induces a gap in the phase-excitation spectrum at the edge of the Brillouin zone. In addition, we show that the gap grows linearly with the field. In contrast to the gap induced by an external magnetic field [18], which can be detected by dielectric measurements, the gap induced by the electric field can be observed only using quasielastic light scattering methods. Although there is experimental evidence hinting towards the existence of the gap [8], precise and unambiguous experimental results are still lacking.

We also investigate the influence of the fluctuations of the phase of the tilt on the dielectric response in a bias electric field in order to understand better the experimental results [9] as well as previous theoretical predictions [10], which contradict each other. The dielectric response to an additional static electric field is calculated for two possible geometries of the sample: for the field to which the response is measured parallel and perpendicularly to the bias field, respectively. For the case of the

field that is parallel to the bias field our numerical results can be compared to the measured ones [9]. Our results are in qualitative agreement with experimental findings; namely, the static susceptibility decreases with the bias field and goes to zero at the critical field. For the case of the field that is perpendicular to the bias field, to our knowledge, no experimental data exist so far.

We show that, as a consequence of a finite system size along the helical axis, two relaxation processes contribute to the static susceptibility. One of these relaxation processes changes the phase of the tilt locally and does not alter the pitch, while the other one is related to the unwinding of the whole helical structure. This last process causes the susceptibility to increase with the field and ultimately diverge at the critical field. This unwinding process is also associated with the relaxation time that increases quadratically with the system length. In the limit of an infinitely large system, our calculation shows that the unwinding process cannot contribute to the dielectric response because the relaxation time needed to unwind the whole helicoidal structure is infinite. Most dielectric as well as optical measurements do not allow for a complete relaxation of the helical structure in order for it to reach an equilibrium. This means that only the local reorientations of the tilt contribute to the measured quantities.

As argued in one of our previous papers [5], the relaxation time related to the unwinding of the helical structure, which depends strongly on the length of the system along the helical axis, can be about three orders of magnitude larger in planar samples compared to homeotropic samples. For example, in a planar sample the length L along the helical axis is usually of the order of 1 cm, which yields the relaxation time related to the unwinding ranging from 1 min to a few hours. Such planar samples are typically used in the critical-electric-field measurements [22] There are two reasons for this: first, the planar geometry allows for an observation of the helical structure under the polarizing microscope and second, it is difficult to apply an electric field parallel to smectic layers in the homeotropic geometry. The slow unwinding process in planar samples can be responsible for the observed first-order character of the Sm-C^*↔Sm-C phase transition, which contradicts the second-order character predicted by the Landau theory [4].

The problem discussed above i.e., the existence of a slow dynamical process that influences the behavior of measured static quantities, is similar to the one in solid ferroelectrics of the type K_2SeO_4, which exhibit a phase transition from the incommensurate to the commensurate phase. The slow dynamical process in this case corresponds to the motion of the domain walls. Similarly, as in the case discussed above, there was a discrepancy between the mean-field predictions [23] and the experimentally observed behavior of the dielectric susceptibility. Holakovský and Dvořak [24] explained this apparent disagreement by assuming that the time-dependent field with the frequency 1 kHz, to which the dielectric response is usually measured, cannot move the domain walls. This assumption lead, as in our case, to a qualitative agreement between theoretically predicted and measured behavior of the dielectric susceptibility.

The phase excitation as calculated in the present work, which changes the period of the modulated structure, cannot change the number of domain walls in the system. Namely, in our description the phase of the tilt changes continuously in space and time. On the other hand, in a real sample the change of the number of domain walls is an activation process; i.e., the system has to overcome a free-energy barrier in order to come to equilibrium [25,26]. From this point of view, the predicted relaxation frequency of the unwinding process, which changes the helical period, is only a rough estimate of the rate at which walls are pushed out of a sample.

ACKNOWLEDGMENTS

The authors thank Dr. Igor Muševič and Dr. Peter Prelovšek for stimulating discussions. We also thank Dr. Luis R. Cruz-Cruz for a careful reading of the manuscript. One of the authors (B.K.U.) acknowledges the support by the Ministry of Science and Technology of the Republic of Slovenia.

APPENDIX: DIELECTRIC RESPONSE OF A FINITE SYSTEM IN A ZERO BIAS FIELD

Here a dielectric response of a system with the length L along the helical axis is investigated in a zero bias field for a general case when there is an arbitrary angle between the time-dependent field $\delta\vec{E} = \delta\vec{E}_0 \cos\omega t$ to which the system responds and the dipole moment $\vec{p}$. Again only the phase Φ of the tilt $\vec{\xi}$ is allowed to vary according to the Landau-Khalatnikov equation (2), where we set $E = 0$. Free boundaries, at $z = 0$ and at $z = L$, yield the boundary conditions $d\Phi/dz\,|_{(z=0)} = q_0$ and $d\Phi/dz\,|_{(z=L)} = q_0$. We can make an ansatz for $\Phi(z,t)$ that already takes into account the boundary conditions

$$\Phi(z,t) = q_0 z + \varphi_0(t) + \sum_{n=1}^{\infty} \alpha_n(t) \cos(n q_m z), \quad \text{(A1)}$$

where $q_m = \pi/L$ is a wave vector associated with the largest possible wavelength allowed in a finite system. The phase φ_0 describes a rigid rotation of the helix as a whole.

The dissipation function $\mathcal{D}$ and the free energy $\mathcal{F}$ can be expanded up to second order in the coefficients $\alpha_n(t)$ and $\varphi_0(t)$

$$\begin{aligned}
\mathcal{D} &= \frac{1}{2}\gamma\Theta^2 L\dot{\varphi}_0^2 + \frac{1}{4}\gamma\Theta^2 L\sum_{n=1}^{\infty}\dot{\alpha}_n^2, \\
\mathcal{F} &= \frac{\pi q_m}{4}K_3\Theta^2\sum_{n=1}^{\infty} n^2\alpha_n^2 \\
&\quad - \frac{2\,\delta E\,P}{q_0}\cos(q_0 L/2 + \varphi_0)\,\sin(q_0 L/2) \\
&\quad - \delta E\,P q_0 \sum_{n=1}^{\infty}\frac{\alpha_n}{q_0^2 - n^2 q_m^2} \\
&\quad \times[(-1)^n\cos(q_0 L + \varphi_0) - \cos\varphi_0]. \qquad \text{(A2)}
\end{aligned}$$

Knowing the dissipation function and the free energy of the system, the Landau-Khalatnikov equations can be expressed as

$$\gamma\Theta^2 L\dot{\varphi}_0 = -\frac{2\,\delta E\,P}{q_0}\sin(q_0L/2)\,\sin(q_0L/2+\varphi_0),$$
$$\frac{1}{2}\gamma\Theta^2 L\dot{\alpha}_n = -\frac{\pi q_m}{2}K_3\Theta^2 n^2\alpha_n + \delta E\,P\,q_0\,\frac{(-1)^n\cos(q_0L+\varphi_0)-\cos\Phi_0}{q_0^2-n^2q_m^2}, \tag{A3}$$

where only the linear terms in δE are considered.

In the absence of the field the phase Φ is a linear function of z, $\Phi = q_0z+\varphi_0$, and φ_0 determines the direction of the dipole moment $\vec{p}$, which is arbitrary, so that in this case the equilibrium state of the system is continuously degenerate (φ_0 can assume any value). In a static electric field the dipole moment $\vec{p}$ turns into the direction of the field, so that $\varphi_0 = m\pi - q_0L/2$, where an integer m is chosen in such a way that the dipole moment $p = |\vec{p}|$

$$p = P\,\frac{(-1)^m\sin(q_0L/2)}{q_0/2} \tag{A4}$$

is positive (m is thus equal to 0 or 1). Instead of $\varphi_0(t)$ we define the angle $\psi_0(t) = \varphi_0(t) - m\pi + q_0L/2$, which is an angle between $\vec{p}$ and the external field $\delta\vec{E}$. The Landau-Khalatnikov equations can be written in a simple form

$$\dot{\Psi}_0 = \frac{\delta E\,P}{\gamma\Theta^2}\kappa_1\sin\psi_0,$$
$$\dot{\alpha}_n = -A_n\,n^2\,\alpha_n - \delta E\,B_n, \tag{A5}$$

where the coefficients A_n and B_n are

$$A_n = \gamma^{-1}K_3\,q_m^2, \tag{A6}$$
$$B_n = \frac{P}{\gamma\Theta^2}\,\frac{2q_0^2}{q_0^2-n^2q_m^2}\times\begin{cases}\kappa_1\sin\psi_0, & n=2k\\ \kappa_2\cos\psi_0, & n=2k+1\end{cases}$$

and the parameters κ_1 and κ_2 are

$$\kappa_1 = (-1)^m\,\frac{\sin(q_0L/2)}{q_0L/2},\quad \kappa_2 = (-1)^m\,\frac{\cos(q_0L/2)}{q_0L/2}. \tag{A7}$$

Taking into account the initial condition $\psi_0(t=0)=\beta_0$, we find the solution for $\psi_0(t)$

$$\psi_0(t) \approx \beta_0 - \frac{\delta E_0\,P\,\kappa_1\,\sin\beta_0}{\gamma\Theta^2\omega}\sin\omega t. \tag{A8}$$

The result (A8) corresponds to a small rigid oscillation of the helix as a whole around an initial position, given by the angle β_0 between the dipole moment $\vec{p}$ and the oscillating field $\delta\vec{E} = \delta\vec{E}_0\cos\omega t$. This response is delayed in phase for $\pi/2$. The amplitudes $\alpha_n(t)$ can be written as sums of two terms: one that is in phase with the external field and another that is delayed for $\pi/2$:

$$\alpha_n(t) = \alpha^0_{n,1}\cos\omega t + \alpha^0_{n,2}\sin\omega t, \tag{A9}$$

where $\alpha^0_{n,1}$ and $\alpha^0_{n,2}$ are

$$\alpha^0_{n,1} = -\frac{\delta E_0\,B_n\,\tau_n}{1+\omega^2\tau_n^2},$$
$$\alpha^0_{n,2} = -\frac{\delta E_0\,B_n\,\omega\,\tau_n^2}{1+\omega^2\tau_n^2} \tag{A10}$$

and the parameter τ_n is equal to $\tau_n = \gamma/(K_3n^2q_m^2)$. The response depends on the initial angle β_0 between $\vec{p}$ and $\delta\vec{E}$. In this case the susceptibility is a 2×2 tensor. One eigenvector is determined by $\beta_0 = 0$ ($\delta\vec{E}\parallel\vec{p}$) and the other one by $\beta_0 = \pi/2$ ($\delta\vec{E}\perp\vec{p}$). The real and the imaginary part of the susceptibility $\chi^{\parallel}_{\rm Re}$ and $\chi^{\parallel}_{\rm Im}$ in the case of $\beta_0 = 0$ and the real and the imaginary part $\chi^{\perp}_{\rm Re}$ and $\chi^{\perp}_{\rm Im}$ in the case $\beta_0 = \pi/2$, respectively, can be expressed in terms of infinite sums

$$\chi^{\parallel}_{\rm Re} = \frac{P}{2E_c}\,l^4\cos^2\left(\frac{\pi l}{2}\right)\times\sum_{k=0}^{\infty}\frac{(2k+1)^2}{[(2k+1)^4+l^4\Omega^2]\,[(2k+1)^2-l^2]^2},$$
$$\chi^{\parallel}_{\rm Im} = \frac{P}{2E_c}\,l^6\,\Omega^2\cos^2\left(\frac{\pi l}{2}\right)\times\sum_{k=0}^{\infty}\frac{1}{[(2k+1)^4+l^4\Omega^2]\,[(2k+1)^2-l^2]^2},$$
$$\chi^{\perp}_{\rm Re} = \frac{P}{2E_c}\,l^4\sin^2\left(\frac{\pi l}{2}\right)\sum_{k=1}^{\infty}\frac{(2k)^2}{[(2k)^4+l^4\Omega^2]\,[(2k)^2-l^2]^2} + \frac{\pi}{8}\frac{P}{E_c}\,\frac{\sin^2(\pi a/2)}{l^2}\,\delta(\Omega),$$
$$\chi^{\perp}_{\rm Im} = \frac{P}{2E_c}\,l^6\,\Omega^2\sin^2\left(\frac{\pi l}{2}\right)\times\sum_{k=1}^{\infty}\frac{1}{[(2k)^4+l^4\Omega^2]\,[(2k)^2-l^2]^2} + \frac{1}{4}\frac{P}{E_c}\,\frac{\sin^2(\pi l/2)}{l^2}\,\frac{1}{\Omega}, \tag{A11}$$

where $l = q_0/q_m = 2L/p_0$ is a dimensionless length of the system and $\Omega = \gamma\omega/(K_3q_0^2)$ is a dimensionless frequency. The expressions in Eq. (A11) can be evaluated explicitly. The analytical result can be derived in the form

$$\frac{\chi^{\parallel}_{\rm Re}}{P/E_c} = \frac{\pi^2}{32}\,\frac{1}{1+\Omega^2}\left[1+\frac{\sin(\pi l)}{\pi l}\right] - \frac{\pi^2}{8}\,\frac{\sin(\pi l)}{\pi l}\,\frac{1}{(1+\Omega^2)^2} - \frac{\pi}{8\sqrt{2}l}\cos^2(\pi l/2)\,\frac{\mathcal{R}^{\parallel}_{+}}{\sqrt{\Omega}(1+\Omega^2)} + \frac{\pi}{4\sqrt{2}l}\cos^2(\pi l/2)\left[\frac{\mathcal{R}^{\parallel}_{+}}{\sqrt{\Omega}} - \sqrt{\Omega}\mathcal{R}^{\parallel}_{-}\right]\frac{1}{(1+\Omega^2)^2},$$

$$\frac{\Omega^{-1}\chi^{\parallel}_{\mathrm{Im}}}{P/E_c} = \frac{\pi^2}{32}\frac{1}{1+\Omega^2}\left[1+\frac{\sin(\pi l)}{\pi l}\right] - \frac{\pi^2}{8}\frac{\sin(\pi l)}{\pi l}\frac{1}{(1+\Omega^2)^2}$$
$$-\frac{\pi}{8\sqrt{2l}}\cos^2(\pi l/2)\frac{\mathcal{R}^{\parallel}_{-}}{\Omega\sqrt{\Omega}(1+\Omega^2)} + \frac{\pi}{4\sqrt{2l}}\cos^2(\pi l/2)\left[\frac{\mathcal{R}^{\parallel}_{+}}{\sqrt{\Omega}} + \frac{\mathcal{R}^{\parallel}_{-}}{\Omega\sqrt{\Omega}}\right]\frac{1}{(1+\Omega^2)^2},$$
$$\frac{\chi^{\perp}_{\mathrm{Re}}}{P/E_c} = \frac{\pi^2}{32}\frac{1}{1+\Omega^2}\left[1+\frac{\sin(\pi l)}{\pi l}\right] - \frac{\pi^2}{16}\frac{\sin(\pi l)}{\pi l}\frac{\Omega^2-1}{(1+\Omega^2)^2}$$
$$-\frac{\pi}{4\sqrt{2l}}\sin^2(\pi l/2)\frac{\sqrt{\Omega}\mathcal{R}^{\perp}_{+}}{(1+\Omega^2)^2} - \frac{\pi}{8\sqrt{2l}}\sin^2(\pi l/2)\frac{(\Omega^2-1)\mathcal{R}^{\perp}_{-}}{\sqrt{\Omega}(1+\Omega^2)^2},$$
$$\frac{\Omega^{-1}\chi^{\perp}_{\mathrm{Im}}}{P/E_c} = \frac{\pi^2}{32}\frac{1}{1+\Omega^2}\left[1+\frac{\sin(\pi l)}{\pi l}\right] + \frac{\pi^2}{8}\frac{\sin(\pi l)}{\pi l}\frac{1}{(1+\Omega^2)^2} - \frac{\pi^2}{16}\frac{\sin^2(\pi l/2)}{(\pi l/2)^2}\frac{1}{\Omega^2}$$
$$-\frac{\pi}{8\sqrt{2l}}\sin^2(\pi l/2)\frac{(\Omega^2-1)\mathcal{R}^{\perp}_{+}}{\Omega\sqrt{\Omega}(1+\Omega^2)^2} + \frac{\pi}{4\sqrt{2l}}\sin^2(\pi l/2)\frac{\mathcal{R}^{\perp}_{-}}{\sqrt{\Omega}(1+\Omega^2)^2}, \tag{A12}$$

where $\mathcal{R}^{\parallel}_{\pm}$ and $\mathcal{R}^{\perp}_{\pm}$ are

$$\mathcal{R}^{\parallel}_{\pm} = \frac{\sinh(\pi l\sqrt{\Omega/2}) \pm \sin(\pi l\sqrt{\Omega/2})}{\cosh(\pi l\sqrt{\Omega/2}) + \cos(\pi l\sqrt{\Omega/2})},$$
$$\mathcal{R}^{\perp}_{\pm} = \frac{\sinh(\pi l\sqrt{\Omega/2}) \pm \sin(\pi l\sqrt{\Omega/2})}{\cosh(\pi l\sqrt{\Omega/2}) - \cos(\pi l\sqrt{\Omega/2})}. \tag{A13}$$

[1] R. B. Meyer, L. Liébert, L. Strzelecki, and P. Keller, J. Phys. Lett. (Paris) **36**, L69 (1975).

[2] See the review article by L. A. Beresnev, L. M. Blinov, M. A. Osipov, and S. A. Pikin, Mol. Cryst. Liq. Cryst. **158A**, 1 (1988).

[3] P. G. de Gennes, *Physics of Liquid Crystals* (Plenum, New York, 1975).

[4] L. Lam and J. Prost, *Solitons in Liquid Crystals* (Springer-Verlag, New York, 1992), Chap. 10.

[5] B. Kutnjak-Urbanc and B. Zekš, Phys. Rev. E **48**, 455 (1993); L. Benguigui and A. E. Jacobs, *ibid.* **49**, 4221 (1994); B. Kutnjak-Urbanc and B. Žekš, *ibid.* **51**, R1569 (1995).

[6] R. Blinc, Ferroelectrics **14**, 603 (1976); R. Blinc and B. Žekš, Phys. Rev. A **18**, 740 (1978).

[7] A. Levstik, T. Carlsson, and B. Žekš, Phys. Rev. A **35**, 3527 (1987); C. Filipič, T. Carlsson, B. Žekš, R. Blinc, F. Gouda, S.T. Lagerwall, and K. Skarp, *ibid.* **38**, 5833 (1988); I. Muševič, R. Blinc, B. Žekš, C. Filipič, M. Čopič, A. Seppen, P. Wyder, and A. Levanyuk, Phys. Rev. Lett. **60**, 1530 (1988); I. Drevenšek, I. Muševič, and M. Čopič, Phys. Rev. A **41**, 923 (1990); A. Levstik, Z. Kutnjak, C. Filipič, and B. Žekš, Ferroelectrics **126**, 139 (1992).

[8] I. Drevenšek, I. Muševič, and M. Čopič, Mol. Cryst. Liq. Cryst. **207**, 199 (1991).

[9] Ch. Bahr, G. Heppke, and N. K. Sharma, Ferroelectrics **76**, 151 (1987); J. Pavel, M. Glogarova, and S.S. Bawa, *ibid.* **76**, 221 (1987).

[10] O. Hudák, J. Phys. (Paris) **44**, 57 (1983).

[11] B. Kutnjak-Urbanc, B. Žekš, and B. Rovšek, Liq. Cryst. **14**, 999 (1993).

[12] B. Žekš, T. Carlsson, I. Muševič, and B. Kutnjak-Urbanc, Liq. Cryst. **15**, 103 (1993).

[13] R. Blinc and B. Žekš, *Soft Modes in Ferroelectrics and Antiferroelectrics* (Elsevier, New York, 1974).

[14] See, e.g., B. Urbanc, B. Žekš, and T. Carlsson, Ferroelectrics **113**, 207 (1991), and references therein.

[15] B. Sutherland, Phys. Rev. A **8**, 2514 (1973).

[16] P. Lebwohl and M. J. Stephen, Phys. Rev. **163**, 376 (1967).

[17] C. Fan, L. Kramer, and M. J. Stephen, Phys. Rev. A **2**, 2482 (1970); J. D. Parsons and C. F. Hayes, *ibid.* **9**, 2652 (1974).

[18] I. Muševič, B. Žekš, R. Blinc, H. A. Wierenga, and Th. Rasing, Phys. Rev. Lett. **68**, 1850 (1992).

[19] P. F. Byrd, and M. D. Friedman, *Handbook of Elliptic Integrals for Engineers and Physicists* (Springer-Verlag, Berlin, 1954).

[20] J. Goldstone, A. Salam, and S. Weinberg, Phys. Rev. **127**, 965 (1962); R. V. Lange, *ibid.* **146**, 301 (1966).

[21] N.W. Ashcroft and N.D. Mermin, *Solid State Physics* (Saunders, Philadelphia, 1976).

[22] S. Dumrongrattana and C. C. Huang, J. Phys. (Paris) **47**, 2117 (1986); A. Levstik, Z. Kutnjak, B. Žekš, S. Dumrongrattana, and C. C. Huang, J. Phys. (France) II **1**, 797 (1991).

[23] P. Prelovšek, J. Phys. C **15**, L269 (1982).

[24] J. Holakovský and V. Dvořak, J. Phys. C **21**, 5449 (1988).

[25] K. Kawasaki, J. Phys. C **16**, 6911 (1983).

[26] P. Prelovšek, Phase Transit. **11**, 203 (1988).